Rev. Roum. Sci. Techn.– Électrotechn. et Énerg.
Vol.**68**, *4*, pp. 363–368, Bucarest, 2023

COMPARISON OF INDUCTIVE AND CAPACITIVE COUPLINGS USED TO CLOSE THE FEEDBACK LOOP USED IN SWITCH MODE POWER SUPPLIES

OVIDIU LĂUDATU[1], MIHAI IORDACHE [1]

Keywords: Capacitive coupling; Inductive coupling; Flyback; Switch mode power supply; Reaction loop.

Switching mode power supplies are widely used to power various electronic equipment and are adaptable to technical requirements. Switching power supplies use average switching frequencies in the kHz-MHz range generated by the internal frequency generator. Switching mode power supplies use one or more feedback reaction loops to stabilize the parameters the connected load requires. We physically realized two switching power supplies using flyback topology to measure the parameters of the two types of couplings, inductive and capacitive. In this article, we presented a comparison of the parameters of the two reaction loops and an analysis of the two modules that make up the reaction loop.

1. INTRODUCTION

Improving switching power supplies must be continuously developed in current research due to their widespread use in most electronic equipment. Switching power supplies (SMPS) are divided into two categories according to the electrical isolation between the source's supply voltage and output voltage. They are divided into power supplies without galvanic isolation and those with galvanic isolation.

Depending on the requirements of the load, the power modules are open-loop, and in this regime, they work as a simple low-frequency transformer at the terminals, the voltage of which is not stabilized. A feedback loop is introduced in the electronic scheme to stabilize the voltage simultaneously with an assurance of the galvanic separation between the output voltage and the input voltage.

An optical coupling using an electronic opt coupler is the most used transfer method to ensure a galvanic separation of the reaction loop. Usually, this is expensive, especially if the working frequency exceeds the value of 5 MHz.

The reaction loop needs such a working frequency, even if it usually works with frequencies of 50 kHz. Due to the duty cycle of the variable signal, problems arise in the case of minimum loads connected to the power source because the duty cycle of the signal is very small, 0.2–0.3 %. In these conditions, reaction loops operating at very high frequencies of 10Mhz are necessary.

To reduce the costs of closing the reaction loop with galvanic separation, it was chosen to replace it with two types of couplings: inductive and capacitive.

They offer very low costs in the production process of the power source compared to the optical coupling. Besides this advantage, both couplings offer significantly higher frequencies than the optical coupling, ensuring galvanic separation at the same time.

In the current modules, in most cases, the feedback loop used to stabilize the output parameters is realized by an optical signal transfer using optocouplers. These insulation components present several disadvantages, both in the short-term and in the long-term operation conditions.

The reaction loop is active all the time the power supply is working. From here, we can deduce that the LED inside the optocoupler is powered continuously or by pulses. The current consumed by it is of the order of 1–5 mA, which represents a high energy consumption in the case of sources where the output power is below 1 W, thus reducing the efficiency of the power source.

Another disadvantage is the temperature range in which the optocoupler works. If the working temperature is very high, it induces delays in the signal or even malfunctions in transmitting the signal.

During the operation of the reaction loop, malfunctions occur in transmitting the signal. In that case, the compensation of the signal in the error amplifier will present erroneous values, which will translate into a very large ripple [8] of the output voltage.

If the optocoupler fails, the PWM generator in the primary module will maintain the fill factor of the signal at the maximum level, resulting in higher voltages at the output of the source than the nominal voltage for which it was designed, from this event destroying the source and the equipment electronics that it powers.

To solve the shortcomings of the optocoupler presented above, we propose replacing it with two types of couplings: inductive and capacitive. These couplers are made from PCB trace (built from FS4 material).

The minimum electrical strength of the typically used FR4 material is 30 kV/mm. Moreover, galvanically insulating coupling elements can be integrated on a PCB by using spiral coils for transformers or plate capacitors for electrical coupling elements very easily. [1] The challenge at this point is to realize a compact and failsafe signal transmission for feedback loop applications with PCB integrated capacitive and inductive coupling elements.

A highly effective planar coil coupler with a wide bandwidth seems to be a promising solution to be implemented for switch mode power supplies, and it offers more flexibility in terms of geometry shapes, size, and turns number, more advantages of the coreless planar inductors can be found [2].

This efficiency highly depends on the position between the transmitting (Tx) and the receiving (Rx) coil and is inversely proportional to the distance between them. Furthermore, an important limiting component of the planar coupler operating frequency bandwidth is the parasitic capacitance, which includes the interface capacitance and the coupling capacitance between the Tx and Rx inductors.

[1] Faculty of Electrical Engineering, the National University of Science and Technology Politehnica of Bucharest.
E-mail: ovidiu.laudatu@stud.electro.upb.ro , mihai.iordache@upb.ro

DOI: 10.59277/RRST-EE.2023.68.4.

Thus, the right compromise must be found between coupling efficiency and the parasitic capacitances, with an optimal model for the designed coupler [2].

Ensuring the closure of the reaction loop used in switching power supplies using a capacitive coupling is an efficient way of achieving galvanic separation between the primary and secondary modules that make up the power supply.

We propose making two capacitors using the PCB route to construct the power supply to realize the capacitive coupling. To realize the capacitors, four copper planes will be designed, two by two, together with the FR4, which represents the dielectric between the two copper planes.

2. INDUCTIVE AND CAPACITIVE COUPLING ELEMENTS

Figure 1 shows the two couplings used to close the reaction loop. On the left side, you can see the two capacitances formed by the PCB path. They make up the electrostatic field coupling. C max- represents the maximum value of the capacity formed for a single capacitor

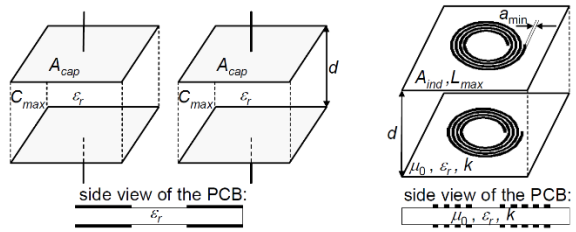

Fig. 1 – Integrated capacitive and inductive loop using PCB traces [1].

A_{cap} represents the area of the armatures that make up the capacitor plates, ε_r the relative permittivity of the dielectric, ε the absolute permittivity of the capacitor dielectric, ε_0 the absolute dielectric permittivity of the vacuum, d the distance between the plates, ε_r the relative permittivity of the dielectric, $\mu_0 = 4\pi \times 10^{-7}$ H/m the permeability of free space, ε_r – the relative permittivity of the dielectric between the two coils, the width of the copper path that forms the coil (mm).

We use the following formula to calculate the capacitance of a single capacitor thus formed from the PCB circuit.

$$C=\frac{Q}{V}=\frac{Q}{V_1-V_2}=\varepsilon\cdot\frac{A\ cap}{d}=\varepsilon_0\cdot\varepsilon_r*\frac{A\ cap}{d}\ [F], \quad (1)$$

$$\varepsilon=\varepsilon_0\cdot\varepsilon_r. \quad (2)$$

On the right side of Fig. 1, you can see the two coils that make up the coupling required to close the reaction loop through inductive coupling. The two coils have a spiral shape. They are arranged on the same plane, the first coil positioned on top of the plane and the other positioned on the bottom.

To calculate the value of the inductance of a coil made from the PCB path, we use (3)

$$L_{max}=\frac{\Phi}{I}[\frac{Wb}{A}]\frac{\mu\cdot(N)^2\cdot S}{l}\ [H], \quad (3)$$

where L_{max} represents the maximum inductance.

The efficiency of the power transfer is given as follows, which shows the dependency of the efficiency on mutual inductance M_0 (5) and resonance frequency ω_0 (4), where R_p and R_s are parasitic resistance of L_1 and L_2, Z_L is the load impedance, ω_0 is the resonant frequency, and M_0 is the mutual inductance between L_1 and L_2 in the air without core [3], k is the coupling coefficient

$$\eta=\frac{Z_L}{(R_s+Z_L)\cdot(1+\frac{R_p(R_s+Z_L)}{(\omega_0\cdot M_0)^2})}, \quad (4)$$

$$M_0=k\sqrt{L_1\cdot L_2}. \quad (5)$$

We need to have a good mutual inductance between the two coils to acquire a good signal transmission.

The coupling coefficient represents the relation between the mutual inductance M and self-inductance's *Lp*, *Ls*. The coupling coefficient of two magnetically coupled systems, the transmitter and receiver for the wireless power transfer system, are as follows [3].

$$k=\frac{\mu_0*M_0}{\sqrt{L_1*L_2}}. \quad (6)$$

For high efficiency, a minimum stable coupling is required. Still, the coupling factor between these air core coils is much lower than the traditional iron core transformer, and it is also highly susceptible to fluctuating under misalignment. Therefore, the coils must be strongly tuned at the same resonance frequency for effective signal transfer while maintaining a minimum coupling factor [3].

3. DIMENSIONING OF INDUCTIVE AND CAPACITIVE COUPLINGS

To simulate and physically realize the two couplings used in the reaction loop, we dimensioned the two capacitors formed with the help of the PCB path and the two coils inductively coupled through the mutual inductance, these being plated top and bottom, ensuring a maximum k coupling.

Table 1 shows the values of a single capacitor consisting of the FR4 PCB dielectric and the two copper plates. Two such formed capacitors will be used in the capacitive coupling.

The value of a single capacitor is 330 pF, a sufficient value to ensure signal stability and compensate for any parasitic capacities between the two modules or between the primary and secondary windings of the transformer.

Table 1

Capacitive couplings

Parameters	Value
Length [mm]	65
Width [mm]	30
Dielectric thickness [mm]	0.2
Thickness of a copper layer [mm]	0.03
Total thickness [mm]	0.26
Capacitance between plate armatures [pF]	330

Table 2 shows the calculated and experimentally measured values of the two magnetically coupled coils formed by the copper layers of the PCB circuit.

Table 2

Inductive couplings

Parameters	Value
RMS voltage (V)	5
C series (pF)	2200
Outer diameter (mm)	33.4
Number of layers	1
Number of turns	10
Coil Width (mm)	0.6
Distance between turns (mm)	0.6
Copper layer thickness (mm)	0.089
Temperature (°C)	25
Inductance (μH)	3.461
LC Resonance Frequency	1.82
(MHz)	0.383
Quality factor Q	0.798
Dc resistance (Ω)	

The two coils ensure the magnetic coupling between the secondary control module and the primary signal reception module. Their design consisted of an analysis of the frequency, their behavior in the magnetic field produced by the power transformer, the current consumed, and the inductance value related to the rise time and the fall time of the signal.

4. SIMULATING THE COMPARISON OF OPTICAL, INDUCTIVE, AND CAPACITIVE COUPLINGS

To study the frequency response of the three couplings, optical - using optocoupler PC817, which is used in most power sources, is a low-cost optocoupler with average performance, capacitive – using two capacitors, inductive using two coils, we propose the simulation of a circuit using the three couplings, having the same signal as input, the circuit was simulated using the Proteus program.

Inductive and capacitive couplings use NPN and PNP bipolar transistors for emission and signal reception modules. The bipolar transistor is a current-controlled semiconductor element. It offers the advantage of base polarization with a relatively small minimum voltage value of ~ 0.7 V.

The relatively low voltage offers the advantage of a reduced number of coil turns in the case of inductive coupling.

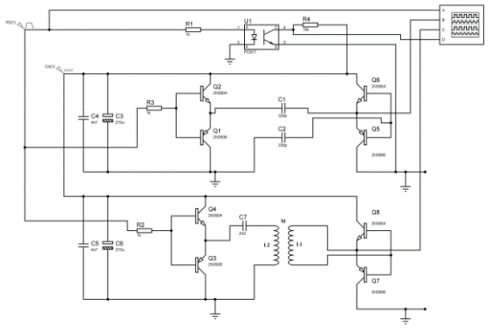

Fig. 2 – Simulate the optical, capacitive, and inductive.

The electronic scheme of the three simulated couplings can be seen in Fig. 2.

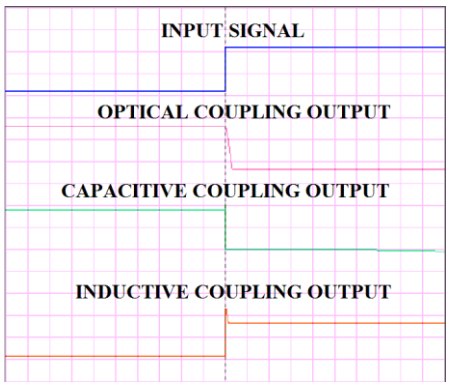

Fig. 3 – The output signals from the three reaction loops.

It is composed of an optocoupler with a pull-up resistor at the output. It forms the optical coupling usually used in switching power supplies. Capacitive and inductive couplings have a class B amplifier as a driver element; it provides the current necessary to power the two couplings. The frequency response of the bipolar transistor is very good compared to the field effect transistor, where delays in signal transmission may occur due to very high parasitic capacitances.

The waveforms of the electronic scheme simulation in Fig. 2 can be seen in Fig. 3. This shows the output signals of the three couplings: optical, capacitive, and inductive coupling. A delay in the falling time can be observed in the case of the optical coupling.

5. EXPERIMENTAL RESULTS

To validate the simulation results, we propose the construction of an experimental electronic circuit using the three couplings. The circuit will help to observe the response times physically, the efficiency of these reaction loops, and also its parameters.

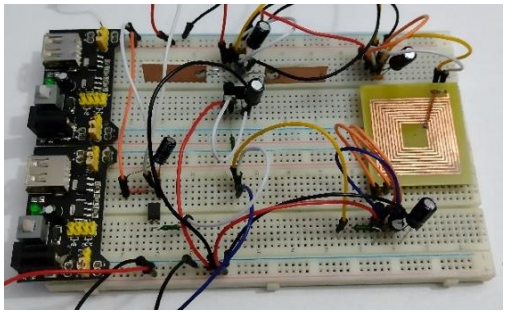

Fig. 4 – The physical realization of the three couplings.

The experimental module can be seen in Fig. 4. It is made on a breadboard module, and it helps to measure the waveform of the current on different paths, making the experimental adaptation of the circuit easier.

To reduce the noise produced by the parasitic inductances, especially on the supply side, we used bypass capacitors connected close to the driver circuits of the couplings, thus limiting the noise produced by the ground plane.

5.1. SIGNAL RESPONSE

Using a four-channel oscilloscope, we made several experimental measurements to determine the response of the reaction loops thus formed and the current consumed by them during signal switching. Using a rectangular signal generator, we transmitted the signal generated simultaneously to the three types of couplings to analyze and compare the output signals.

The first analysis of the output signals can be seen in Fig. 5, using a frequency value used in most flyback converters of 50 kHz, having a rectangular waveform of the signal, simulating a variable filling factor of the signal, we chose a minimum value of Dt of 1 %. The duty cycle of 1 % and 50 kHz gives us a response of the reaction loop with a frequency of 5 MHz.

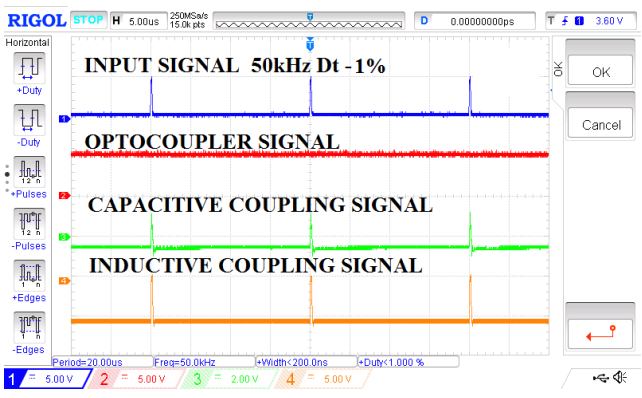

Fig. 5 – Optical, capacitive, and inductive signal low Dt, output measurements.

We can observe that the reaction loop, using the optical PC817 coupling, did not respond to the frequency of 5 MHz.

The filling factor with a value of 1% is used by switching power supplies when they are in no-load conditions. In this case, the reaction loop must respond to the order of MHz so that the output voltage value does not present a ripple, nor does the driver module do pulse skipping.

Suppose the reaction loop does not respond and pulse skipping intervenes. In that case, the source will also generate a signal from the audio range due to the avalanche current from the primary winding.

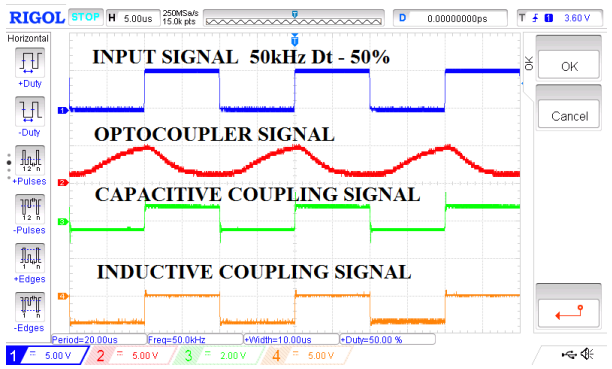

Fig. 6 – Optical, capacitive, and inductive signal maximum Dt, output measurements.

Most power supplies using the flyback topology use a duty cycle of 5 0% maximum of the primary winding command signal to ensure a current mediation between the semiconductor element in the primary and the rectifier diode or the rectifier transistor in the secondary module. Operating with a filling factor of 50 % means the source is in maximum load or overload conditions. In these conditions, the reaction loop must ensure the transfer of the signal from the secondary module to the primary module.

We generated a 50 kHz signal with a duty cycle of 50 % to check the operation under load or overload conditions. This measurement can be seen in Fig. 6. We can observe that the optical coupling reaction loop fails to ensure the optimal transmission of the signal, presenting long delays for the rising and falling times.

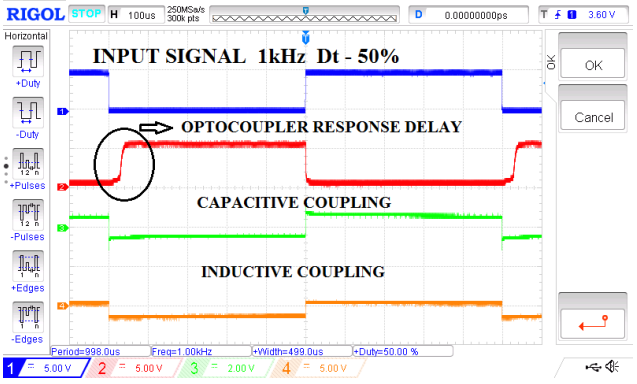

Fig. 7 – Optical coupling delay using PC817 optocoupler.

To compare the response of the reaction loop through optical coupling versus capacitive and inductive couplings, we reduced the frequency value to 1 kHz. You can see in Fig. 7 a delay of the rising time of the signal of ~50 ns. This is due to the parasitic parallel capacitance inside the LED of the optocoupler.

5.2. COMPARISON OF SIGNAL DELAYS BETWEEN INDUCTIVE AND CAPACITIVE REACTION LOOP

We notice above that using a common optocoupler PC817 to transmit the rectangular signal from the secondary module to the primary module introduces large delays both on the rising time and on the falling time and does not represent a viable solution for a reaction loop that requires a bandwidth of the order of MHz.

We can deduce that the two solutions for closing the reaction loop through capacitive and inductive coupling are viable. To compare the performances of the two reaction loops, we made two measurements: the first measurement for the rising time of the signal, which can be seen in Fig. 8, and the second measurement for the falling time of the signal, which can be seen in Fig. 9.

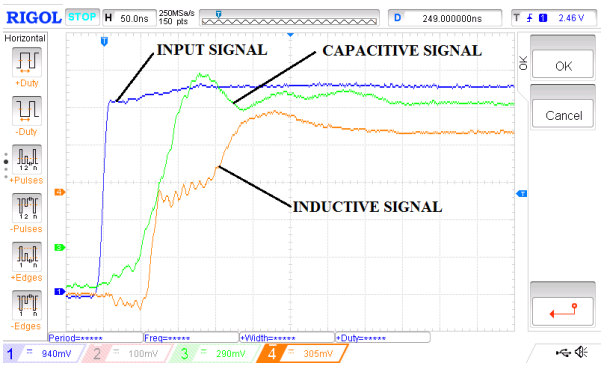

Fig. 8 – The comparison between capacitive coupling and inductive coupling during the rising time.

Analyzing the signal response in Fig. 8, we can deduce that the capacitive coupling presents a slower delay than the inductive coupling, which was to be expected due to the capacitive reactance at high frequencies. If we consider a threshold voltage of 1 V, we can see that the response frequency of the capacitive coupling is higher than that of the inductive coupling, which presents a delay of ~ 60 ns.

The high frequency that can be observed at half the rising time of the inductive coupling is due to the polarization of the bipolar transistor and the back EMF effect presented by the inductive coupling. To reduce this effect, snubber circuits can be used. They will be considered in future studies.

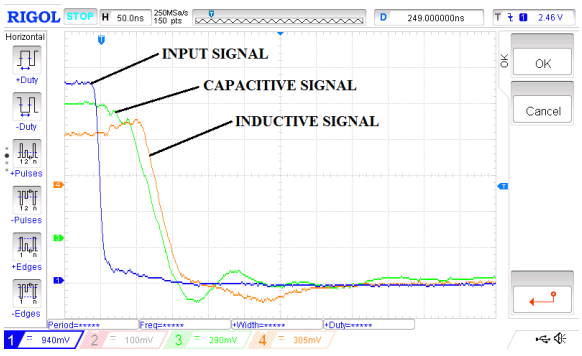

Fig. 9 – The comparison between capacitive coupling and inductive coupling during the falling time

In Fig. 9, we can observe the falling time of the reaction loop signal; we can see that the capacitive coupling signal has a delay time compared to the fundamental signal, which is smaller than the inductive coupling. Considering a minimum control voltage of 1 V, the capacitive coupling has a delay time of 70 ns and the inductive coupling of 80 ns. In

other words, we can deduce that the capacitive coupler's response time is better during the signal's falling time.

Comparing the two signals from Fig. 7 and Fig. 8, we can deduce that the inductive coupling has a total delay time of 70 ns compared to the capacitive coupling.

The total delay of the signal deduced from the two measurements using the capacitive coupling with the minimum command voltage of 1 V is ~130 ns. In inductive coupling, the total delay of the rising and falling times compared to the fundamental signal is ~145 ns.

5.3. CURRENT CONSUMPTION OF THE REACTION LOOP

The signal transmitted by the reaction loop, using the pulse control from the secondary module, is rectangular. To switch the rising and falling times, the reaction loops, using inductive and capacitive coupling, need only a pulse to change the logic state of the signal.

From here, we can conclude that the energy consumed by the two loops using capacitive or inductive couplings is lower than that consumed by optical coupling, where the LED must be fed in constant mode or by long-lasting pulses.

To analyze the current pulses required to supply the driver circuit, both for the inductive and the capacitive coupling, we made two measurements where the current pulses can be observed, both for the falling and rising times.

We used two resistors with a value of 1 Ω as a shunt for the measurements. It was connected between the ground and the driver circuit so that we could simultaneously measure the current consumed by the reaction loop, both for the inductive and capacitive coupling. Thus, we can infer the current value by reading the voltage on the shunt resistor.

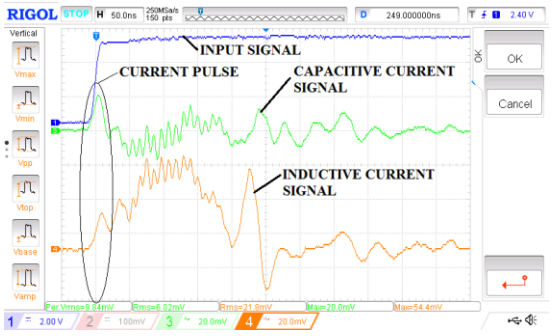

Fig. 10 – The current pulse consumed by the reaction loop for the rising time of the signal.

Figure 10 shows the eight waveforms of the current the driver circuit consumes to control the reaction loop. In the case of the capacitive coupling, we can observe an I_{rms} = 6.02 mA of the total current, including the parasitic couplings., having a maximum current pulse value of 20.05 mA, sinusoidal waveform, with a duration of ~25 ns. In the inductive case, we can see that the back EMF voltage affects the current waveform, resulting in a slightly higher value than in the case of capacitive coupling. It is expected to have these oscillations due to the inductive nature of the coupling without a high-frequency attenuation circuit. These oscillations also appear because of the LC coupling between the transmission coil and the CB capacity of the bipolar transistor. Inductive coupling requires a current pulse of ~21 mA, like capacitive coupling.

In Fig. 11, the waveforms of the current consumed by the circuit to switch the signal during the falling time can be analyzed. In the case of capacitive coupling, we can observe a current with a value of 20 mA, which is necessary to change the state of the signal. In the case of inductive coupling, we can observe a lower value of ~19 mA.

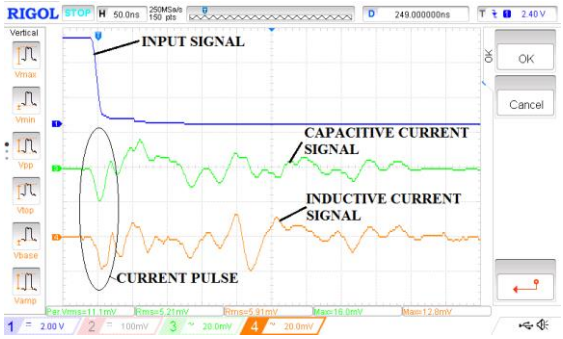

Fig. 11 – The current pulse consumed by the reaction loop for the falling time of the signal.

The pulse duration, both for capacitive coupling and for inductive coupling, is ~25 ns. After the current pulse, some ringing can be observed after switching due to the inductivities present in the circuit.

Analyzing the measurements made to measure the consumed current, we can deduce that the consumed current values are almost identical in the designed and physically realized circuit. Both couplings show very good energy efficiency during rising and falling times.

6. USING THE CAPACITIVE AND INDUCTIVE REACTION LOOP IN THE FLYBACK TOPOLOGY

To verify the functionality of the reaction loop, we experimentally created two switching power supplies, using the two couplings analyzed above to close the reaction loop.

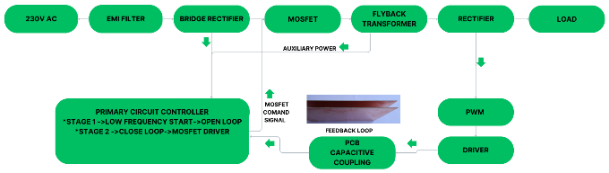

Fig. 12 – Switch mode power supply using feedback loop through capacitive coupling.

Figure 12 shows the block diagram of the switching power supply using the flyback topology. Through capacitive and inductive coupling, only alternating signal components can be transmitted. For this reason, for the module in the secondary to receive energy, the power source must start in an open loop and then switch to a closed loop through inductive or capacitive coupling.

The primary module is a specialized circuit with the role of a PWM generator and driver for the power transistor. In the secondary module, there is the main PWM controller, which transmits the pulses through the reaction loop to the primary module, thus closing the reaction loop.

The advantage of the PWM circuit in the secondary is that it ensures a much faster response to variable loads connected to the source. This translates into a low ripple of the source.

Figure 13 shows the power source that contains the inductive coupling for closing the reaction loop. It is similar in principle to the power source in Fig. 12. In this case, the closing of the reaction loop is done by inductive coupling using the two planar coils.

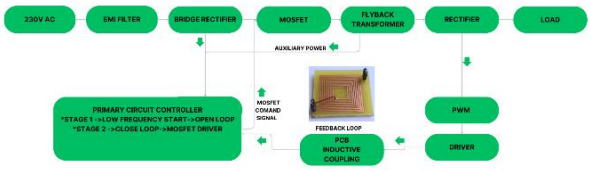

Fig. 13 Switch mode power supply using feedback loop through inductive coupling.

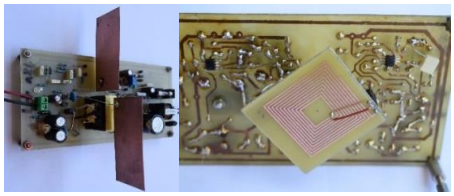

Fig. 14 – The physically built switch mode power supply using the two couplings.

The physical realization of the two power sources using the two couplings can be seen in Fig. 14. On the left side, you can see the two capacitive couplings made experimentally from the PCB circuit using FR4. On the right side, you can see the two coils that make up the inductive coupling, which ensures the closing of the reaction loops through inductive coupling.

7. **CONCLUSIONS**

Analyzing the above, we can conclude that inductive and capacitive couplings offer enough advantages to be used in the design of switching power supplies. They offer advantages such as high working frequencies, low energy consumption, and low production costs compared to current electronic circuits that use analog and digital optocouplers. The capacitative coupling has the advantage of a very high working frequency, higher than inductive coupling. To make the capacitive coupling, two copper layers of the PCB circuit, or four copper layers connected two by two in parallel, to mitigate the parasitic capacities that appear between the module in the secondary and the module in the primary.

These capacities can induce some parasites in the signal but not so much as to disturb the functionality of the reaction loop. The breakdown voltage is not very high, so we cannot ensure a very high galvanic separation voltage through capacitive coupling. This coupling time is acceptable where there are no large variations in parasitic capacity between the secondary and the primary, for example, in an LED light bulb or a battery charging module. Inductive coupling has a slightly delayed response compared to capacitive coupling. Still, the response is quite good regarding ns, considering that the typical rising time for a field effect transistor is ~200 ns from the cause of parasitic capacitances.

The inductive coupling ensures a breakdown voltage of the galvanic isolation much higher than that of the capacitive coupling. For this reason, it should be used for power supply modules where the supply voltages are 80 V–2 kV. Both couplings offer an energy efficiency worthy of consideration, especially in the case of the design of very low power supply sources.

ACKNOWLEDGMENTS

The results presented in this article have been funded by the Ministry of Investments and European Projects through the Human Capital Sectoral Operational Program 2014-2020, Contract no. 62461/03.06.2022, SMIS code 153735.

Received on 14 November 2023

REFERENCES

1. S. Zeltner, *Insulating IGBT driver with PCB integrated capacitive coupling elements*, International Conference on Integrated Power Electronics Systems (CIPS), pp. 1–6, 16–18 March 2010.
2. A. Allioua, G. Griepentrog, M. Vogel, J. Eitler, N. Mahdavi, *Design of PCB-based planar coil inductive coupler*, IEEE Annual Southern Power Electronics Conference (SPEC), pp. 1–8, 6–9 Dec. 2021.
3. M. Mostak, S. Kwak, S. Choi, *Core design for better misalignment tolerance and higher range of wireless charging for HEV*, Annual IEEE Conference on Applied Power Electronics Conference and Exposition (APEC), pp. 1748–1755, 12 May 2016.
4. C.P. Zheng, N.Y. Dai, M.C. Wong, C.K. Wong, M. Zhu, *Capacitive-coupling inverter for PV integration: Analysis and implementation*. Proceedings of the 2014 9th IEEE Conference on Industrial Electronics and Applications (ICIEA), pp. 666–671 (2014).
5. J. Xiong, T. Wei, T. Luo, Q. Tan, C. Xue, J. Liu, W. Zhang, *Coupling influence on signal readout of a dual-parameter LC resonant system*, Advances in Mathematical Physics, pp. 1–9 (2015).
6. J. Zhang, S. Yao, L. Pan, Y. Liu, C. Zhu, Chunbo. *A review of capacitive power transfer technology for electric vehicle applications*. Electronics. **12**, p. 3534 (2023).
7. P. Athira, T.Z. Ang, M. Salem, Mohamed, *Resonant inductive coupling for wireless power transmission*. International Journal of Energy and Power Systems, **2**, pp. 1–5 (2022).
8. H. Sridharan, S. Ramalingam, J. Arumugam, *Wide boost ratio in quasi-impedance network converter using switch voltage spike reduction technique*, Rev. Roum. Sci. Techn.– Électrotechn. et Énerg. **68**, *3*, pp. 259–265 (2023).